^{13}C NMR Studies of Wheat Germ Agglutinin Interactions with *N*-Acetylglucosamine at a Magnetically Oriented Bilayer Surface†

Brian J. Hare,‡ Frode Rise,§,‖ Yves Aubin,§,⊥ and James H. Prestegard*,§

Department of Chemistry and Department of Molecular Biophysics and Biochemistry, Yale University, New Haven, Connecticut 06511

Received March 14, 1994; Revised Manuscript Received June 15, 1994®

ABSTRACT: The orientation of synthetic ^{13}C-labeled glycolipid receptors and their interaction with the plant lectin wheat germ agglutinin have been studied in an oriented membrane system using NMR spectroscopy. A series of 2-[1,2-$^{13}C_2$]acetamido-2-deoxy-β-D-glucopyranosides were synthesized with between zero and four hydrophilic ethoxy units between the headgroup and an alkyl chain which anchors the receptors in the bilayers. The chemical shift anisotropy of the ^{13}C carbonyl and a ^{13}C–^{13}C dipolar coupling between the labeled carbons provide information about the orientation and dynamics of the receptor headgroup in oriented membrane systems. It was found that the headgroups of the receptors with two, three, or four ethoxy units appeared isotropic when incorporated in the oriented bilayers, but those of the receptors with zero or one ethoxy units were significantly ordered by the bilayers. The average orientations consistent with measured spectral parameters were determined for the receptors with zero and one ethoxy units and were found to coincide with low-energy conformations from molecular modeling. When the plant lectin wheat germ agglutinin was added to the sample, only the receptors with two, three, or four ethoxy units separating the headgroup from the alkyl chain showed evidence of binding by the lectin. Although the ^{13}C-labeled resonances broadened when the protein bound, no changes in dipolar couplings or chemical shift anisotropies could be detected, suggesting that the motion of the headgroup was slowed by protein binding, but average orientation and overall order changed little. Competition studies demonstrated that none of the lectin/receptor complexes are more stable than the complex of the lectin and *N*-acetylglucosamine in solution. These results suggest that the membrane does not stabilize the interactions of wheat germ agglutinin with these cell-surface receptors. Furthermore, molecular modeling demonstrates that the zero- and one-spacer receptors may not bind wheat germ agglutinin because the orientations of the *N*-acetyl groups in these receptors would result in significant steric contacts between the lectin/receptor complex and the membrane.

A wide variety of biological processes are mediated by interactions between carbohydrates and proteins at the surfaces of membranes. These include the initial step in infection of a host cell by bacteria or viruses (Lingwood, 1992; Sharon & Lis, 1993), differentiation of cells during embryogenesis (Feizi, 1985), and oncogenic cellular transformation (Hakomori, 1991). Soluble lectins from plants were the first sugar-specific binding proteins to be discovered, and the molecular basis for their interactions with sugars and their biological functions remain active areas of research (Lis & Sharon, 1991; Hoekstra & Düzgunes, 1989). More recently, lectins and proteins with lectin-like domains have been discovered in mammals, including humans. The known functions of these molecules include endocytosis of glycoproteins, complement-mediated lysis of pathogens as well as the recently characterized adhesion of leukocytes to endothelial cells as part of the inflammatory response (Drickamer, 1988, 1993; Mayadas et al., 1993; Lasky, 1992; Hughes, 1992). Increasing evidence suggests that the conformational properties of cell-surface carbohydrates are likely to be important determinants of the recognition events which confer specificity upon these processes (Ladisch et al., 1992; Strömberg et al., 1991). Therefore, the development of methods for the study of carbohydrates at the surfaces of membranes and their application to systems of biological interest have become important research targets. We present here an application of some relatively new NMR[1] methodology to the study of lectin–glycolipid interactions at the surface of a model membrane.

Information about the structures of cell-surface complexes has been difficult to obtain. High-resolution NMR has provided information about the conformation and dynamics of oligosaccharides in solution (Bush, 1992; Homans & Rutherford, 1993; Poppe et al., 1992) as well as thermodynamic and kinetic parameters for protein/carbohydrate complexes (Kronis & Carver, 1985a,b). High-resolution NMR methods have also been applied to membrane-bound complexes by incorporating them in very small micelles or unilamellar vesicles (Henry & Sykes, 1992; Shon et al., 1991). Resolution, however, is limited by broad lines, and relaxation-based structural analysis is difficult because cross-relaxation among the myriad of protons in a membrane-like environment makes conversion of NOEs to distance constraints susceptible to errors

† Financial support from the National Institutes of Health (GM 33225) to J.H.P., from the Royal Norwegian Council for Scientific and Industrial Research to F.R., and from the Ministère de l'Education du Québec to Y.A. is gratefully acknowledged.

‡ Department of Molecular Biophysics and Biochemistry.

§ Department of Chemistry.

‖ Present address: Department of Chemistry, University of Oslo, P.O. Box 1033 Blindern, N-0315 Oslo, Norway.

⊥ Present address: Department of Biochemistry, The Hospital for Sick Children, 555 University Ave., Toronto, Ontario M5G 1X8, Canada.

® Abstract published in *Advance ACS Abstracts,* August 1, 1994.

[1] Abbreviations: DMPC, L-α-dimyristoylphosphatidylcholine; CHAPSO, 3-[(chloamidopropyl)dimethylammonio]-2-hydroxyl-1-propanesulfonate; NMR, nuclear magnetic resonance; WGA, wheat germ agglutinin; NOE, nuclear Overhauser effect; TLC, thin-layer chromatography; PDB, Protein Data Bank.

0006-2960/94/0433-10137$04.50/0

of interpretation. The structures of a number of complexes between proteins and carbohydrates have also been solved by X-ray crystallography (Kjellen & Lindahl, 1991; Vyas, 1991). Crystallization in the presence of a lipid matrix, however, has been notoriously difficult.

An alternative approach relies on NMR observation but employs an array of phospholipid/detergent bilayers which spontaneously orient in magnetic fields (Sanders et al., 1994). A nondenaturing detergent, 3-(cholamidopropyl)dimethylammonio-2-hydroxyl-1-propanesulfonate (CHAPSO), and the phospholipid dimyristoylphosphatidylcholine (DMPC) are used. The system appears to be composed of uniformly dispersed bilayer disks in which surfaces closely approximate those of more extended, pure lipid bilayers. This approach has some advantages over solution NMR. Since the bilayers are oriented, dipolar couplings, quadrupolar couplings, and chemical shift anisotropies, which are averaged to zero in solution, are observed. These parameters can be easily measured for samples enriched in ^{13}C and contain information about the orientation and dynamics of the molecule of interest.

The NMR observations are analogous to those of more conventional solid-state NMR methods. These methods have been successfully applied to structural analyses of glycolipids anchored at membrane surfaces (Winsborrow et al., 1992) and to structural analysis of transmembrane peptides (Ketchem et al., 1993) using arrays of lipid multilayers either randomly dispersed or mechanically oriented between glass plates. Since the small, flat disks in the DMPC/CHAPSO system are well dispersed, the surfaces are more readily accessed by proteins added to the samples. Typically, 70–80% of the weight of the sample is water, so soluble proteins are easily accommodated. In comparison to solid-state NMR using randomly dispersed samples, relatively narrow lines, instead of a powder pattern, are observed.

A number of NMR active nuclei might be used as probes of glycolipid behavior. Protons offer high sensitivity when either monitored directly or used for indirect detection of other nuclei. However, because of the large background ^1H signal from the DMPC/CHAPSO bilayers and extensive dipolar coupling among protons in the liquid crystal media, methods for ^1H detection of unlabeled molecules incorporated in the bilayers are difficult to apply. ^{13}C NMR offers higher resolution but at the expense of lower sensitivity. Enrichment in ^{13}C of the molecule of interest offers significant improvements in sensitivity as well as the opportunity to differentiate molecules of interest from the significant natural abundance background of the lipid matrix. Enrichment can be done using uniform biosynthetic labeling, but, even with the inherent resolution offered by ^{13}C NMR, this often leads to degeneracy of resonances. Here we employ a synthetic strategy, allowing labeling and detection of specific sites. ^{13}C nuclei are also incorporated in coupled pairs, allowing double-quantum spectroscopy. Detection of pairs of ^{13}C spins further differentiates the labeled molecule because only 1 pair of carbons in 10 000 in a natural abundance sample have the ^{13}C isotope as both members of the pair.

Here, we have chosen to investigate the feasibility of employing labeled systems containing the *N*-acetyl functionality. We have previously reported the use of a triply-labeled fragment as a part of a sialic acid ring (Aubin & Prestegard, 1993), but the occurrence of acetyl groups is more widespread. The influenza virus hemagglutinin and selectins as well as many plant lectins recognize 2-acetamido-2-deoxyglucoside (*N*-acetylglucosamine) or 5-acetamidoneuraminic acid (sialic acid). The *N*-acetyl group plays an important role in recognition of sialic acid by influenza virus hemagglutinin (Sauter et al., 1992) and in the recognition of *N*-acetylglucosamine and sialic acid by wheat germ agglutinin (Bhavanandan & Katlic, 1979; Monsigny et al., 1980; Wright, 1990).

We report here a novel synthesis of glycolipid analogs containing a doubly ^{13}C-labeled *N*-acetylglucosamine headgroup separated from a lipid chain by a variable-length hydrophilic spacer group. The strategy of synthesizing glycolipid analogs with hydrophilic spacers has been used before to determine how far the headgroup must extend into solution to interact with a soluble lectin (Hampton et al., 1980; Slama & Rando, 1980; Sundler, 1984). In our case, orientation and dynamics of the headgroup may be monitored by using NMR to directly observe the ^{13}C-labeled acetyl group.

A doubly ^{13}C-labeled acetyl moiety, incorporated synthetically into *N*-acetylglucosamine, potentially contains a great deal of structural information. Assuming axially symmetric motion of the headgroup, the ^{13}C–^{13}C and ^{13}C–^1H dipolar couplings, D_{ij}, measured between the ^{13}C-labeled carbonyl and methyl carbons or between the labeled carbons and nearby protons may be written as follows:

$$D_{ij} = \frac{-\gamma_i\gamma_j}{2\pi^2 r^3} S_{\text{micelle}} S_{\text{axial}} \left(\frac{3\cos^2\theta - 1}{2} \right) \qquad (1)$$

γ_i and γ_j are the gyromagnetic ratios of the two interacting nuclei, S_{micelle} is an order parameter describing the average orientation and order of lipids in the bilayer fragments, and S_{axial} is an order parameter describing the degree of motional disorder of the glycolipid headgroup relative to its membrane anchor. The angle θ is the average angle between a given internuclear vector *ij* and the bilayer normal. The bond length r is determined from the fixed geometry of the headgroup, and S_{micelle} may be determined from independent NMR measurements as described previously (Sanders & Prestegard, 1992). Therefore, the only variable parameters in eq 1 are the order parameter S_{axial} and the angles θ_{ij}.

Additional information is available in a labeled *N*-acetyl group from chemical shift anisotropy. The deviation of the observed chemical shift of a nucleus from its isotropic value, $\delta_{\text{anisotropic}}$, in a molecule undergoing axially symmetric motion is given by

$$\delta_{\text{anisotropic}} = -\frac{2}{3} S_{\text{micelle}} S_{\text{axial}} \left(\delta_{zz} - \frac{1}{2}\delta_{yy} - \frac{1}{2}\delta_{xx} \right) \qquad (2)$$

where S_{axial} and S_{micelle} are the same order parameters described above, and δ_{zz}, δ_{yy}, and δ_{xx} are the diagonal elements of the chemical shift tensor written in a frame with the z axis coincident with the bilayer normal. For any orientation of the headgroup, δ_{zz}, δ_{yy}, and δ_{xx} can be calculated by transforming the chemical shift tensor. When combined with values for S_{axial} and S_{micelle}, chemical shifts can be predicted. Average orientations which are consistent with experimental data are found by rotating the headgroup about its torsional degrees of freedom, calculating coupling constants and chemical shift anisotropies which are scaled by S_{axial} for each structure, and comparing to the measured parameters. More complete analyses of the orientation and order of glycolipid headgroups which do not rely on the assumption of axial symmetry have been described elsewhere (Aubin & Prestegard, 1993; Hare et al., 1993; Sanders & Prestegard, 1991).

In order to demonstrate the usefulness of the *N*-acetyl labeled group in structural studies of carbohydrates and the compatibility of the oriented DMPC/CHAPSO system for

studying protein interactions with carbohydrates at a membrane surface, we report here the results of studies of the interaction of the labeled glycolipid analogs with the plant lectin wheat germ agglutinin. Plant lectins, including wheat germ agglutinin, are thought to function by binding carbohydrates present on membrane surfaces, such as cell-surface carbohydrates of invading pathogens. Furthermore, it is known that wheat germ agglutinin induces the fusion of vesicles containing gangliosides (Redwood & Polefka, 1976), suggesting that the protein itself might interact with the bilayer. A high-resolution crystal structure of the lectin complexed with sialic acid has been reported (Wright, 1990) as well as a great deal of biophysical data characterizing the interaction of the lectin with a variety of carbohydrates in solution. Since the natural cell-surface ligands of WGA have not yet been determined, however, the role of the bilayer in stabilizing cell-surface complexes is unknown. The molecules used in this study offer the opportunity to explore the structure and dynamics of cell-surface carbohydrates complexed to WGA at a variety of distances from the bilayer surface.

MATERIALS AND METHODS

Materials

3-[(Cholamidopropyl)dimethylammonio]-2-hydroxyl-1-propanesulfonate (CHAPSO), L-α-dimyristoylphosphatidylcholine (DMPC), and wheat germ agglutinin (WGA) were purchased from Sigma Chemical Co. (St. Louis, MO). WGA was purchased and used as a mixture of isolectins. Doubly labeled acetyl chloride was purchased from Cambridge Isotopes Laboratories (Woburn, MA). Ethylene glycol monotetradecyl ether (oxyethylene 1-myristyl ether) and diethylene glycolmonotetradecyl ether (polyoxyethylene 2-myristyl ether) were purchased from Fluka Chemie AG (CH 9470, Buchs, Switzerland). All other reagents used in preparation of the NMR samples and used in the synthesis of the glucosides were purchased from Aldrich Chemical Co. (Milwaukee, WI).

Synthesis

The synthesis of the receptors is outlined in Figure 1.

Synthesis of 2-[1,2-$^{13}C_2$]Acetamido-2-deoxy-α,β-D-glucopyranose 1,3,4,6-Tetraacetate (3). Compound **2** was obtained from glucosamine hydrochloride and doubly ^{13}C-labeled *N*-acetylsuccinimide using the selective *N*-acetylating procedure of Whitesides (Heidlas et al., 1992a,b). The doubly-labeled *N*-acetylsuccinimide is easily obtained from doubly-labeled *N*-acetyl chloride and hydroxysuccinimide (Heidlas et al., 1992a). Prior to use in the preparation of glycoconjugates, the remaining hydroxyl groups in **2** were protected using standard peracetylation procedures.

Synthesis of [2-^{13}C]Methyl(3,4,6-tri-O-acetyl-1,2-dideoxy-α-D-glucopyrano)-[2,1-d]-[2-^{13}C]oxazoline (4). The anomeric site of **3** was activated for glycoside formation by preparation of the oxazoline (**4**). 2-[1,2-$^{13}C_2$]Acetamido-2-deoxy-α,β-D-glucopyranose 1,3,4,6-tetraacetate (**3**) (1.00 g, 2.555 mmol) was dissolved in dry dichloroethane (4 mL, Aldrich Sure Seal), molecular sieves (4 Å, 100 mg) were added, and the reaction flask was flushed with dry argon gas. TMS triflate (0.89 mL, 4.34 mmol, 1.7 equiv) was added, and the reaction was stirred at room temperature for about 1 h, until the reaction had halted as judged by TLC (silica, diethyl ether/methanol, 100:2; sample made alkaline with triethylamine before application). Triethylamine (4 mL) was added, stirred for 1 min, and the solvent evaporated. The product was purified, and the unreacted 2-[1,2-$^{13}C_2$]acetamido-2-deoxy-α-D-glucopyranose

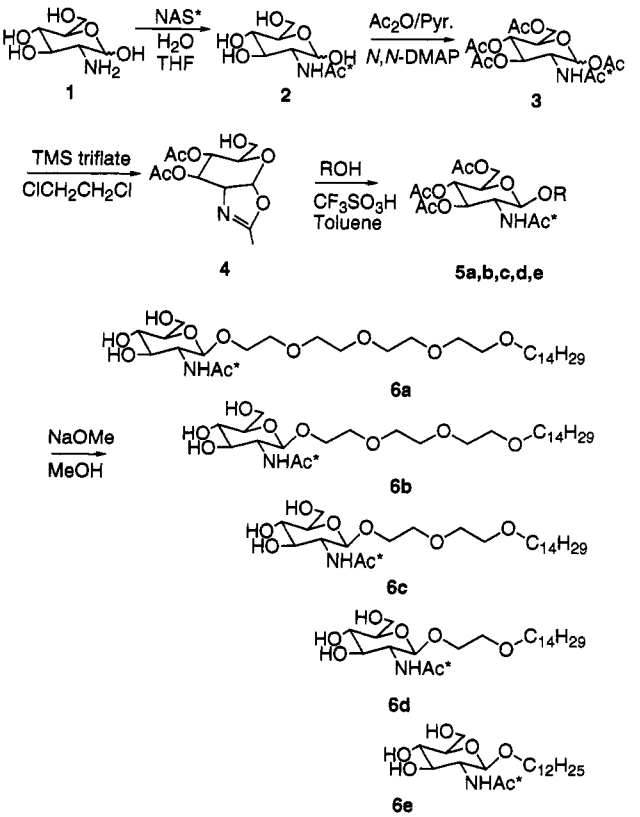

FIGURE 1: Synthesis of ^{13}C-labeled four-, three-, two-, one-, and zero-spacer receptors for wheat germ agglutinin. An asterisk (*) denotes molecules containing a doubly ^{13}C-labeled acetyl group. Abbreviations: NAS, *N*-acetylsuccinimide; THF, tetrahydrofuran; NHAc, *N*-acetyl; Ac_2O, acetic anhydride; Pyr, pyridine; *N,N*-DMAP, 4-dimethylaminopyridine; AcO, O-acetyl; TMS triflate, trimethylsilyl trifluoromethanesulfonate; NaOMe, sodium methoxide; MeOH, methanol.

1,3,4,6-tetraacetate (α-**3**) was recovered by flash chromatography (silica, diethyl ether/methanol, 50:1 and 9:1). Yield (**4**): 0.4233 g (1.282 mmol, 50.2% [94.7% based on recovered α-**3**]). Oily material. ^1H NMR ($CDCl_3$, 250 MHz): d 1.81 and 2.33 (2 d, 3H, NHCOC$\underline{H}_3$, J $^{13}\underline{C}H$ 130.2 Hz, J $^{13}\underline{C}^{13}\underline{C}H$ 7.3 Hz), 2.05 (s, 3H, CH_3), 2.07 (s, 3H, CH_3), 2.09 (s, 3H, CH_3), 3.58 (m, 1H, H5), 4.11 (broad m, 1H, H2), 4.15 (d, 2H, H6, J_{HAHB} 4.4 Hz), 4.90 (d, 1H, H4, J 9.2 Hz), 5.24 (broad s, 1H, H3), 5.95 (dd, 1H, H1, J_{H1H2} 7.4 Hz, $J_{H1}{}^{13}{}_{C1}$ 4.6 Hz). High-resolution mass spectrum for $^{13}C_2{}^{12}C_{12}H_{20}NO_8$ (M + 1): Calcd, 332.1256; found, 332.1259. Recovered α-**3** 0.9777 g (1.201 mmol, 47.0%). Oily material. It was concluded that only the β anomer readily cyclized at room temperature. Yet raising the temperature of the α/β mixture of **3** led to the formation of undesired side products.

Cyclization of Recovered 2-[1,2-$^{13}C_2$]Acetamido-2-deoxy-α-D-glucopyranose 1,3,4,6-Tetraacetate (α-3). To avoid side products, the α isomer was separated as described above and treated separately as follows. 2-Acetamido-[1′,2′-$^{13}C_2$]-2-deoxy-α-D-glucopyranose 1,3,4,6-tetraacetate (α-**3**) (0.3252 g, 0.831 mmol) was dissolved in dry dichloroethane (4 mL, Aldrich Sure Seal), molecular sieves (4 Å, 50 mg) were added, and the reaction flask was flushed with dry argon gas. TMS triflate (0.29 mL, 1.413 mmol, 1.7 equiv) was added, and the reaction was stirred at 60 °C for 1 h, until the reaction had halted as judged by TLC (silica, diethyl ether/methanol, 100:2; sample made alkaline with triethylamine before application). Additional TMS triflate (0.29 mL, 1.413 mmol, 1.7 equiv) was added, and the mixture was stirred for one more hour at 60 °C when all starting material had been consumed as judged

by TLC. Triethylamine (4 mL) was added and stirred for 1 min, and the solution was evaporated. The product was purified by flash chromatography (see above). Yield (**4**): 0.263 g (95.8%). The combined yield from α and β anomers of **3** was 95%. Spectroscopic data for **4**: see above.

*Synthesis of Dodecyl 2-[1,2-$^{13}C_2$]Acetamido-3,4,6-tri-O-acetyl-2-deoxy-β-D-glucopyranoside (**5e**).* Since all syntheses of peracetylated alkyl glycosides (**5**) were similar, only the method for **5e** will be described. [2-^{13}C]Methyl(3,4,6-tri-*O*-acetyl-1,2-dideoxy-α-D-glucopyrano)-[2,1-*d*]-[2-^{13}C]oxazoline (**4**) (0.3518 g, 1.062 mmol) and dodecanol (1.978 g 10.617 mmol) were dissolved in dry toluene (20 mL, Aldrich Sure Seal) under an argon atmosphere. Trifluoromethanesulfonic acid (93.9 mL, 0.106 mmol) was added and the mixture heated to 60 °C. TLC (silica, diethyl ether/methanol, 50:1; sample made alkaline with triethylamine before application) 1 h after the addition of the acid showed approximately 50% conversion of the oxazoline. Trifluoromethanesulfonic acid (4 mL) was added to reinitiate the reaction. Pyridine (4 mL) was added to the mixture after 30 min, and the solvent was evaporated. Toluene (5 mL) was added, and the solvent was evaporated once more. This procedure was repeated four times. The product was purified by flash chromatography (silica gel, diethyl ether/methanol, 98:2; diethyl ether/methanol, 9:1). Yield (**5e**): 0.2718 g (49.5%). Oily material. ^{1}H NMR ($CDCl_3$, 250 MHz): d 0.88 (t, 3H, CH_3, dodecyl), 1.25 (s, 20H, dodecyl), 1.57 (bt, 2H, CH_2, C_{11}, dodecyl), 1.68 and 2.19 (3H, $NHCOCH_3$, J_{CH} 128.1 Hz, J_{CH} 6.1 Hz), 2.02, (3H, CH_3), 2.03 (3H, CH_3), 2.08 (3H, CH_3), 3.41–3.51 (m, 1H, OCH_2, dodecyl), 3.66–3.73 (m, 1H, H5), 3.77–3.89 (m, 2H, H2 + OCH_2, dodecyl), 4.09–4.30 (m, 2H, H6), 4.68 (d, 1H, H1, J_{H1H2} 8.3 Hz), 5.06 (t,[dd] 1H, H4, J_1 9.7 Hz, J_2 9.5 Hz), 5.31 (dd, 1H, H3, J_1 9.5 Hz, J_2 9.3 Hz), 5.46 (broad d, 1H, NH). Five equivalents of the appropriate ethylene glycol monotetradecyl ether were used to prepare **5b**, **5c**, **5d**, and **5e**.

*Synthesis of Dodecyl 2-[1,2-$^{13}C_2$]Acetamido-2-deoxy-β-D-glucopyranoside (**6e**).* Again, the deacetylation of all alkyl glycosides was similar, so the procedure for the dodoecyl analog (**6e**) is described. Dodecyl 2-[1,2-$^{13}C_2$]acetamido-3,4,6-tri-*O*-acetyl-2-deoxy-β-D-glucopyranoside (**5e**) (0.2718 g, 0.525 mmol) was dissolved in methanol (15 mL), cooled to 0 °C, and purged with argon. Four drops of sodium methoxide (Janssen 16.860.79, 30 wt %) were added, and the solution was stirred for 24 h while gradually warming to ambient temperature. Silica gel (5 g) was added, and the methanol was evaporated. The dry silica gel was applied to the top of a flash chromatography column, and the product was obtained by eluting with a gradient starting with diethyl ether and ending with methanol. Yield, 99%; mp, 169–170 °C. ^{1}H NMR (CD_3OD, 300 MHz): d 0.88 (t, 3H, CH_3), 1.27 (bs, 10H, dodecyl), 1.51 (q, 2H, CH_2), 1.73 and 2.16 (dd, 3H, CH_3, $NH^{13}CO^{13}CH_3$, J_{CH} 128.2 Hz, J_{CH} 6.1 Hz), 3.23–3.87 (several m, 6H, H2, H3, H4, H5, H6), 4.35 (d, 1H, H1, J_{H1H2} 8.5 Hz). Isotopic labeling was verified with NMR spectroscopy and high-resolution mass spectrometry. Results of the mass spectrometry are as follows:

*Dodecyl 2-[1,2-$^{13}C_2$]Acetamido-2-deoxy-β-D-glucopyranoside (**6e**).* High-resolution mass spectrum for $^{13}C_2{}^{12}C_{18}H_{39}NO_6$ (M + 1): Calcd, 392.2923; found, 392.2936.

*1-Myristyloxyethylenyl 2-[1,2-$^{13}C_2$]Acetamido-2-deoxy-β-D-glucopyranoside (**6d**).* High-resolution mass spectrum for $^{13}C_2{}^{12}C_{22}H_{47}NO_7$ (M + 1): Calcd, 464.3497; found, 464.3457.

*2-Myristylpoly(oxyethylenyl) 2-[1,2-$^{13}C_2$]Acetamido-2-deoxy-β-D-glucopyranoside (**6c**).* High-resolution mass spectrum for $^{13}C_2{}^{12}C_{24}H_{51}NO_8$ (M + 1): Calcd, 508.3762; found, 508.3763.

*3-Myristylpoly(oxyethylenyl) 2-[1,2-$^{13}C_2$]Acetamido-2-deoxy-β-D-glucopyranoside (**6b**).* High-resolution mass spectrum for $^{13}C_2{}^{12}C_{26}H_{55}NO_9$ (M + 1): Calcd, 552.4024; found, 552.4021.

*4-Myristylpoly(oxyethylenyl) 2-[1,2-$^{13}C_2$]Acetamido-2-deoxy-β-D-glucopyranoside (**6a**).* High-resolution mass spectrum for $^{13}C_2{}^{12}C_{28}H_{59}NO_{10}$ (M + 1): Calcd, 596.4284; found, 596.4294.

Thus, we produced five glycolipid analogs with a variable hydrophilic tether, allowing a systematic structural investigation of the WGA interaction with receptors at different distances from the bilayer surface.

Preparation of DMPC/CHAPSO NMR Samples

The liquid crystalline NMR samples were prepared directly in 5-mm diameter NMR tubes. The appropriate receptor (1.18 μmol) was added as a solution in methanol, the sample was evaporated *in vacuo*, and 136 μmol of DMPC, 45 μmol of CHAPSO, and 329 μL of buffer (58 mM KH_2PO_4, 14 mM K_2HPO_4, 150 mM NaCl, pH 6.1) were then added. The samples had a lipid content of 27% (w/v). The sample was then sealed with teflon tape and capped. A combination of hand centrifugation, heating, cooling, and sonication was utilized to obtain an optically clear, homogenous sample. A complete description of the oriented DMPC/CHAPSO liquid crystals has been described elsewhere (Sanders & Prestegard, 1990). Up to 0.29 μmol of wheat germ agglutinin dimer was added as a lyophilized powder to a homogeneous liquid crystal sample. Concentrations of WGA are calculated based on a dimer molecular mass of 34 kDa (Nagata & Burger, 1974). The lectin was distributed uniformly through the sample by hand centrifugation.

NMR Methods

The NMR spectra of the liquid crystals were recorded on a Bruker AM500 and a GE Omega NMR spectrometer, operating at 125.67 MHz for ^{13}C. Spectra were recorded at 40 °C, unless otherwise noted, without a field frequency lock. ^{1}H heterodecoupling, using WALTZ-16 with 40 W of power, was performed during the acquisition of 2K real data points. An acquisition time of 35 ms and a repetition delay of 1.3 s minimized heating of the sample. Double-quantum filtered spectra were acquired using 1D INADEQUATE pulse sequences (Bax et al., 1981) with the same acquisition parameters as above. Again, ^{1}H heterodecoupling was employed during evolution and acquisition. The ^{1}H spectrum of *N*-acetylglucosamine was recorded on a GE Omega 500 spectrometer with an S-17 gradient accessory. The data sets were processed using FELIX version 2.10 (Biosym Technologies, San Diego). INADEQUATE spectra were fit to Lorentzian lines using the simplex algorithm to minimize the square of the error in order to determine their widths. The line width and intensity of each peak in each antiphase pair was fit separately, and the resulting line widths were averaged.

Molecular Modeling

The energy maps used in this study were generated using AMBER 4.0 (Pearlman et al., 1991). The starting structures of the map were generated by a tree search of ϕ and ψ torsion angles at 20° intervals using the MULTIC option of Mac-

romodel V3.1 (Still, 1990). Each structure was minimized using the Macromodel version of the MM2 force field with the glycosidic torsions ϕ and ψ constrained to the starting values. The minimized structures were used as PDB overlays in the EDIT module of AMBER and further minimized to convergence, constraining ϕ and ψ and using a convergence criterion for the norm of the energy gradient of 0.01 kcal mol^{-1} A^{-1}. In the AMBER minimizations, ϕ and ψ were constrained and a force field with improved paramaterization for oligosaccharides was utilized (Scarsdale et al., 1988). Partial charges for the carbohydrate ring atoms used in the AMBER minimization are the same as those used previously (Scarsdale et al., 1988), and the oxyethylene oxygen and its lone pairs were assumed to have identical charges as the C1 oxygen of the sugar. The partial charges for the *N*-acetyl group were taken from estimates of partial charges on a peptide backbone (Weiner et al., 1986).

Agglutination Assays

Five vesicle solutions were prepared by sonicating 30 mg of a mixture of DMPC with 5 mol % of one of the five ^{13}C-labeled glycolipid analogs. The solutions were sonicated in a 10-mm diameter NMR tube at 40 °C in a Branson E-module ultrasonicator at 40 kHz (350 W) for about 15 min in 5 mL of buffer (58 mM KH_2PO_4, 14 mM K_2HPO_4, 150 mM NaCl, pH 6.1) until the solution was clear. Varying amounts of WGA were added to 1 mL of a solution containing 100 μg of vesicles, and absorbance at 450 nm was determined after incubation for 10 min at room temperature with a Zeiss UV/vis spectrophotometer (Model M4 QII 3083).

The aqueous and lipid phases of the zero- and four-spacer samples were separated by centrifugation in a Beckman air-driven ultracentrifuge at 170000*g* for 2 h to determine whether the lectin-bound receptor was attached to the lipid bilayer. Lectin concentration in the aqueous phase was assayed in a Hewlett Packard 8451A diode array spectrophotometer. UV absorption curves between 220 and 350 nm were fit to a linear combination of lectin and vesicle absorption spectra using the simplex algorithm and minimizing the square of the error. The aqueous and lipid phases of the four-spacer receptor were separated by spinning at 170000*g* and 15 °C using a Beckman L8-M ultracentrifuge and a 60 Ti rotor to determine whether the WGA in the aqueous phase bound a significant fraction of the receptor.

RESULTS

A methodology based on the oxazoline chemistry illustrated in Figure 1 allowed the synthesis in reasonable yield of five glycolipid analogs with varying numbers of oxyethylene units between the *N*-acetylglucosamine headgroup and the alkyl chain. The oxyethylene units are believed to be reasonably hydrophilic and should remain in the aqueous phase above the bilayer interface. Therefore, varying the number allows a systematic investigation of the effect of membrane proximity on receptor conformation and on lectin binding. The methyl and carbonyl carbons of the acetate in the headgroups are ^{13}C labeled. NMR spectroscopy may be used to monitor the headgroup orientation both alone in the membrane phase and interacting with WGA.

Orientation and Dynamics of Isolated Receptors. Spectra of the four-spacer receptor which was doubly labeled in ^{13}C and incorporated in DMPC/CHAPSO at 40 °C are shown in Figure 2. The ^1H-decoupled ^{13}C NMR spectrum is shown in Figure 2a, and the corresponding ^1H-decoupled ^{13}C NMR spectrum with double-quantum filtration using the 1D

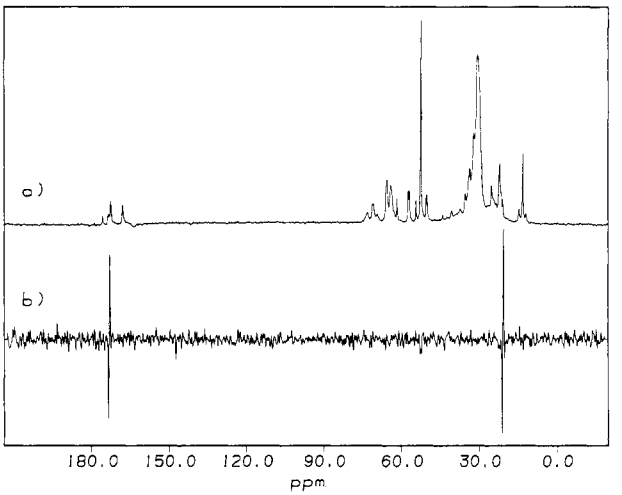

FIGURE 2: (a) ^1H-decoupled, inverse-gated ^{13}C NMR spectrum of 2.6 mM four-spacer receptor ^{13}C labeled in the acetyl carbons. The receptor is in 3:1 DMPC/CHAPSO with 28% (w/v) lipid content in phosphate buffer. The spectrum was acquired at 40 °C with 3600 scans, and it was processed using 2 Hz of linebroadening. (b) Double-quantum filtered 1D INADEQUATE spectrum of the same sample with the same acquisition and processing parameters as in spectrum a.

INADEQUATE pulse sequence is shown in Figure 2b. The two labeled *N*-acetyl carbons resonate at 20 and 170 ppm. They are difficult to identify, however, in the directly observed spectrum because of interference from natural abundance signals from the liquid-crystal matrix. The two resonances are clearly identified in the INADEQUATE spectrum (Figure 2b) as antiphase pairs. The splitting of each antiphase doublet is the sum of dipolar coupling and scalar coupling. In this case, the observed coupling is near the scalar value of 50 Hz.

Variations in the coupling constants and chemical shifts of the various receptors incorporated in the DMPC/CHAPSO preparation are shown in the stacked plot of ^1H-decoupled ^{13}C NMR spectra in Figure 3. The doublet from the *N*-acetyl carbonyl of the four-spacer receptor is observed in Figure 3a at 174.8 ppm. Other resonances belong to the *sn*-1 phospholipid carbonyl at 169.5 ppm, the *sn*-2 phospholipid carbonyl at 174.0 ppm, and the CHAPSO carbonyl at 177.3 ppm. The *sn*-1 carbonyl is shifted significantly upfield from its isotropic position of 174 ppm because of incomplete averaging of chemical shift anisotropy in the oriented medium. Its position provides an internal control on overall order of the liquid crystal matrix. The ^{13}C–^{13}C splitting of the acetate is again near the scalar value of 50 Hz, and the chemical shift is near its isotropic value of 174.6 ppm.

As the number of oxyethylene spacers in the receptor is reduced from four to zero in Figure 3, the spectra undergo a number of changes. The carbonyl resonance shifts downfield for the shorter spacers, away from the isotropic value, indicating greater order of the headgroups which are closer to the bilayer. The resonance of the zero-spacer receptor is broad, probably indicating some heterogeneity in the samples containing this receptor. The coupling constants and chemical shifts for the two-, three-, and four-spacer receptors and the chemical shifts of the zero- and one-spacer receptors were measured directly from the spectra shown in Figure 3.

The coupling constants for the zero- and one-spacer receptors were measured from the methyl regions of the spectra corresponding to those in Figure 3. Data for the one-spacer receptor are shown in Figure 4. The small resolved coupling of 10 Hz observed in Figure 4a is a sum of scalar and dipolar contributions. As the degree of order in the sample used for

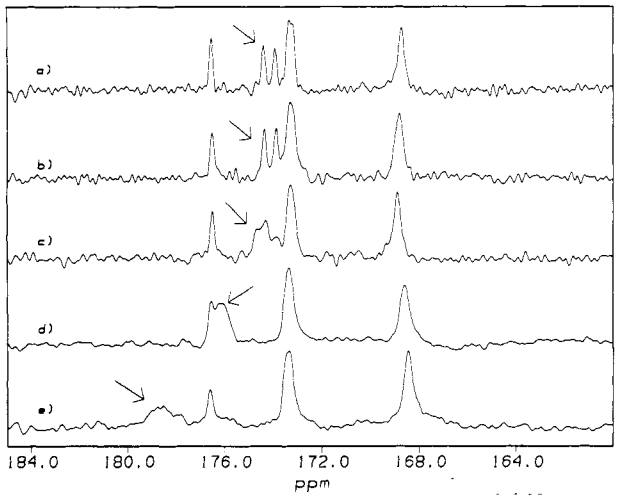

FIGURE 3: ^{1}H-decoupled, inverse-gated ^{13}C NMR specta of 2.6 mM receptor ^{13}C labeled in the acetyl carbons. The carbonyl regions of the spectra are shown. The receptors are in 3:1 DMPC/CHAPSO with 28% (w/v) lipid content in phosphate buffer. The four-spacer receptor is shown in spectrum a, the three-spacer receptor in spectrum b, the two-spacer receptor in spectrum c, the one-spacer receptor in spectrum d, and the zero-spacer receptor in spectrum e. The arrow in each spectrum points to the resonance assigned to the labeled carbonyl in the receptor. Additional resonances are from natural abundance ^{13}C in the lipid matrix. The spectra were acquired at 40 °C with 3600 scans. Spectra a–c were processed using 3 Hz of linebroadening, while spectra c and d were processed using 20 Hz of linebroadening. The digital resolution of each spectrum after zero-filling to 8K complex points is 7.2 Hz/point.

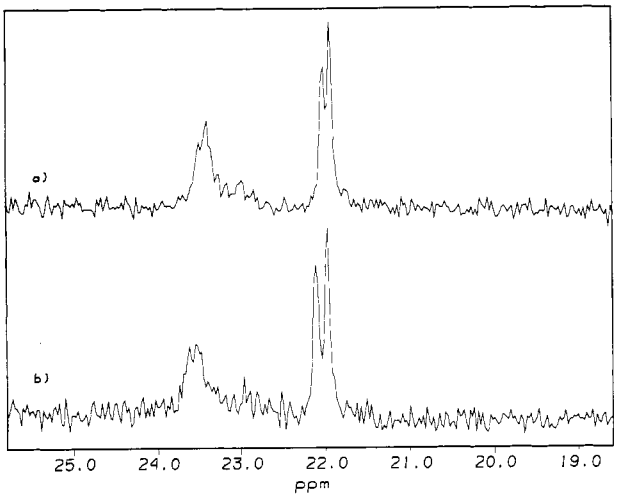

FIGURE 4: ^{1}H-decoupled, inverse-gated ^{13}C NMR spectra of 7.4 mM one-spacer receptor ^{13}C labeled in the acetyl carbons. The methyl regions of the spectra are shown. The receptor is in 3:1 DMPC/CHAPSO with 28% (w/v) lipid content in phosphate buffer. Spectrum a was acquired at 40 °C, and spectrum b was acquired at 32 °C. Both spectra were processed using –0.5 Hz of exponential linebroadening. The digital resolution of each spectrum after zero-filling to 8K complex points is 6 Hz/point.

the spectrum in Figure 4b was reduced by lowering the temperature, the coupling increased toward the scalar value of 49 Hz, suggesting that the dipolar contribution to the coupling observed in Figure 4a is –39 Hz. If the coupling had been observed to decrease through a null and then increase toward the scalar value as a result of reduced system order, a dipolar coupling of –59 Hz would have been indicated. Table 1 summarizes the anisotropic chemical shift and the observed dipolar coupling constants of the various receptors. The signs of the dipolar coupling constants relative to the scalar coupling constants were determined by methods similar to those shown in Figure 4.

Table 1: Dipolar Coupling Constants and Chemical Shift Anisotropies for Receptors

receptor	dipolar coupling (Hz)	chemical shift anisotropy ($\Delta\delta$/ppm)
four-spacer	5 ± 10	0.3 ± 0.2
three-spacer	15 ± 10	0.3 ± 0.2
two-spacer	5 ± 10	0.5 ± 0.2
one-spacer	–40 ± 10	2.1 ± 0.4
zero-spacer	–90 ± 20	3.8 ± 0.4

The dipolar coupling and chemical shift anisotropy for the zero-spacer and one-spacer glycolipid analogs depart significantly from isotropic values, demonstrating that these receptors are significantly ordered by the bilayer. These data can be used to screen models for allowed orientation and dynamics of the headgroup. The program WIGNER5 has been used to determine the orientation and dynamics of β-dodecyl glucoside in DMPC/CHAPSO bilayers from dipolar and quadrupolar coupling data (Hare et al., 1993). A module was added to WIGNER5 which calculates the chemical shift of each orientation of the headgroup using eq 2. Briefly, it rotates the rigid headgroup of a glycolipid about its torsional degrees of freedom and calculated dipolar couplings and chemical shift offsets at each point. It is assumed that the orientation of the headgroup is determined by the torsion angles ϕ and ψ, defined as O5–C1–O1–C1′ and C1–O1–C1′–C2′, respectively. Here, C1′ and C2′ refer to the two carbons in the oxyethylene spacer. The remainder of the oxyethylene chain and the acyl chain are assumed to undergo axially symmetric motion. The calculated values are compared to experimental values and pairs of torsion angles are saved if the calculated and measured parameters agree within experimental error.

The structure of the *N*-acetylglucosamine headgroup of the receptors was taken from an X-ray crystal determination (Mo & Jensen, 1975). The H–N–C_2–H torsion angle connecting the *N*-acetyl group to the glucose backbone, however, is not necessarily the same as in the crystal structure or may not even be rigid in the molecules anchored in the lipid bilayers. We therefore measured the HN–H2 vicinal ^{1}H coupling constant across this torsion angle in a 40 mM solution of *N*-acetylglucosamine in 10% D_2O/acetate buffer (10 mM sodium acetate, 150 mM acetic acid, pH 3.5) using a 1D gradient-enhanced jump–return spin echo sequence (Plateau & Guéron, 1982). The measured value of 8 Hz is consistent with the crystal structure torsion angle of 140° (Pardi et al., 1984). Since both crystal and solution results are the same, it seems reasonable to restrict the torsion angle to its crystal structure value in our calculations.

Since data are limited to a dipolar coupling and a chemical shift anisotropy value, a very simple model for motional averaging had to be assumed. WIGNER5 allows a number of models for motional averaging to be used, including simple axially symmetric averaging (see eq 1). While most glycolipids are known to execute nonaxially symmetric motion, it has been shown in at least one case that average conformations are not highly sensitive to this assumption (Sanders & Prestegard, 1991). A value for $S_{micelle}$ of –0.20 was taken from ^{2}H spectroscopy of β-dodecyl glucoside deuterated at the position connecting the acyl chain to the glucose headgroup (Sanders & Prestegard, 1991). The order parameter S_{axial}, then, will account for motional disorder of the oxyethylene unit and the *N*-acetylglucosamine headgroup. S_{axial} should be roughly comparable to the principal order parameter S_{zz} calculated for simple alkyl glycoside headgroups in previous studies.

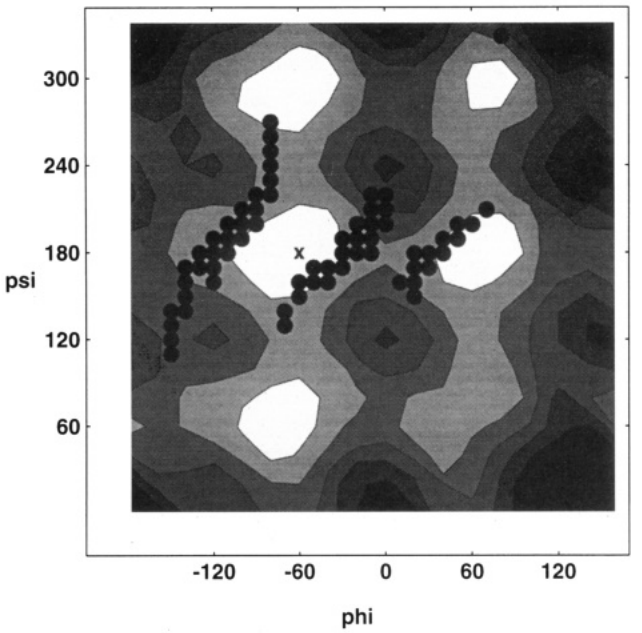

FIGURE 5: Experimental solutions for the average orientation of the one-spacer receptor headgroup superimposed on a potential energy map of the headgroup generated by AMBER, which shows energy as a function of the glycosidic torsion angles. The black dots are average orientations of the headgroup which are consistent with the experimental data. The X marks the global minimum energy structure based on molecular modeling. Lighter shades correspond to lower-energy regions in the map. The contours are spaced 2 kcal/mol apart.

The principal values of the ^{13}C carbonyl tensor and the orientation of the principal axes were taken from the experimentally determined ^{13}C carbonyl chemical shift tensor for glycinylglycine hydrogen chloride monohydrate (Oas et al., 1987). The principal values for δ_{11}, δ_{22}, and δ_{33} are 244, 171, and 95 ppm, respectively, referenced to TMS. Two tensor axes in the diagonalized frame for this molecule, corresponding to the principal values δ_{11} and δ_{22}, are oriented in the peptide plane, and δ_{22} is aligned approximately along the C=O bond. The orientation of the principal axis corresponding to δ_{33} is nearly perpendicular to the peptide plane. Significant variations are observed for the principal values and orientations of the principal axes among different peptides (Oas et al., 1987). Since the line width in our samples limits the accuracy of our measurement of experimental parameters to about 10%, however, the relatively small variations observed in the chemical shift tensors should not limit the precision with which our structures can be defined.

Average structures which are consistent with our experimental data were determined by incrementing the torsion angles ϕ and ψ by 1° between 0° and 360° and the order parameter S_{axial} by 0.05 between 0 and 1. Figure 5 shows the solutions which are consistent with the data for the one-spacer glycolipid analog as black dots superimposed upon a potential energy map generated by AMBER (Pearlman et al., 1991). The plot was produced at lower resolution (10° steps in ϕ and ψ) but accurately reflects the distribution of most solutions. The regions of the map displayed with lighter shades correspond to lower-energy conformations. The solutions cluster primarily into three groups, centered at $\phi = -110°$, $\psi = 180°$, $\phi = -30°$, $\psi = 180°$, and $\phi = 50°$, $\psi = 180°$. The order parameter for the headgroup, S_{axial}, ranges between 0.15 and 0.75. The order parameters for all but a few solutions were less than 0.5. Additional solutions near $\phi = 80°$, $\psi = 330°$ are in a higher-energy region of the potential energy map and are not shown in Figure 5. The order parameter for these solutions ranges from 0.90 to 1.0, unreasonably high in comparison to the average order parameter for the other three sets of solutions and data on other glycolipids. Solutions for the zero-spacer glycolipid were found to cluster in nearly identical groupings, but with S_{axial} ranging between 0.3 and 1.0 for the three sets of solutions nearest the minima of the potential energy map (data not shown).

A major limitation of the force field used in the modeling in Figure 5 is that no attempt was made to account for the effect of the membrane surface on the energy of the molecule. In an attempt to include the membrane in the energy modeling, an energy term used previously by our group to describe the interaction of the glycolipid with its surroundings in the vicinity of a lipid/water interface was included in the target function of AMBER (Ram et al., 1993). However, when the glycolipid was positioned such that the oxygen connecting the oxyethylene unit to the acyl chain was at the midpoint of the variable dielectric function representing the bilayer, the membrane energy term differed by no more than 1.5 kcal/mol among all the conformations generated by rotating the glycolipid about the ϕ and ψ torsion angles. No changes were found in the position of the global minimum or any of the local minima in the energy map.

Interaction of Wheat Germ Agglutinin with the Receptors. The plant lectin WGA could be stably incorporated into samples containing the four-spacer receptor in concentrations up to a 1:4 molar ratio between WGA dimer and the receptor. Significant association of WGA with the four-spacer receptor in our samples is supported by the observation that higher stoichiometric concentrations of WGA could not be incorporated even when receptor concentrations were decreased by a factor of 2, suggesting that association with the receptor is necessary for stable incorporation of WGA into these samples. These results are consistent with each WGA dimer binding to four carbohydrate ligands in our sample, which was also the stoichiometry observed in solution NMR studies between sialic acid and WGA (Kronis & Carver, 1985b).

Samples containing the three-spacer receptor or two-spacer receptor could be made homogeneous and optically clear at a 1:4 molar ratio between WGA dimer and the receptor, but the samples became cloudy after several hours, indicating separation of the sample into heterogeneous phases. Lower concentrations of WGA could be incorporated, however, in samples with the three-spacer and two-spacer receptors. Even WGA concentrations corresponding to a 1:4 molar ratio between WGA dimer and receptor could not be stably incorporated into samples containing the one-spacer or zero-spacer receptors. These samples were still prepared, however, and NMR spectra were acquired as rapidly as possible.

Figure 6 shows the 1D ^{13}C NMR spectra of the receptors in the presence of WGA in the oriented lipid system. Comparison with the spectra in Figure 3 shows that the addition of WGA to the two-, three-, and four-spacer receptors broadens the carbonyl resonance but does not change the chemical shift significantly. The ^{13}C–^{13}C coupling constant cannot be determined in these spectra because the lines are too broad. These results are consistent with the WGA binding the receptors and slowing their motion, but not affecting their overall order. The zero- and one-spacer receptors appear unperturbed by the binding of WGA. The addition of WGA does not appear to affect the orientation or order of the DMPC/CHAPSO bilayers, since a comparison of Figures 3 and 6 shows that the resonances due to natural abundance ^{13}C carbonyls in DMPC and CHAPSO (170, 174, and 177 ppm) do not change position when WGA is added.

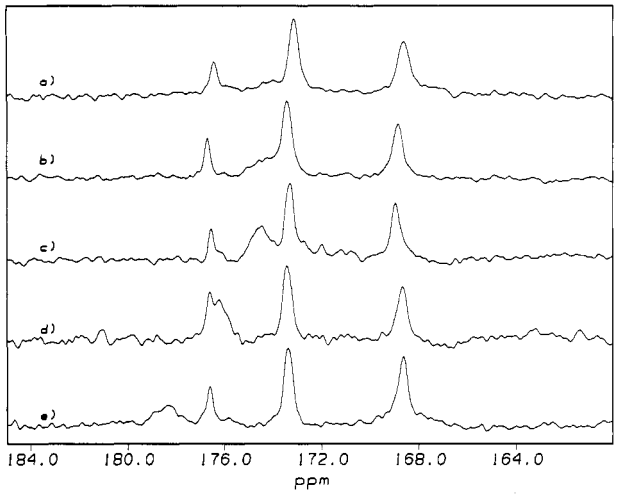

FIGURE 6: ^{1}H-decoupled, inverse-gated ^{13}C NMR specta of 2.6 mM receptor ^{13}C-labeled in the acetyl carbons in the presence of the plant lectin WGA. The carbonyl regions of the spectra are shown. The receptors are in 3:1 DMPC/CHAPSO with 28% (w/v) lipid content in phosphate buffer. The samples with the four-spacer receptor and three-spacer receptor in spectra a and b, respectively, each contain 0.65 mM WGA dimer. The samples with the two-spacer receptor, one-spacer receptor, and zero-spacer receptor in spectra c, d, and e, respectively, each contain 0.22 mM WGA dimer. The spectra were acquired at 40 °C with 3600 scans and were processed using 20 Hz of linebroadening.

Spectra of samples with less than stoichiometric amounts of WGA and the four-spacer receptor show spectra intermediate between those in Figures 3 and 6 (data not shown). Since the lines broaden monotonically with increasing WGA content, but the area under the lines remains the same, the data suggest the receptor is exchanging rapidly on the NMR time scale between the bound and unbound states. The dissociation rate between WGA and sialic acid in solution is consistent with the rapid exchange observed in these experiments (Kronis & Carver, 1985a).

Determination of Equilibrium Dissociation Constants. For a receptor exchanging rapidly on the NMR time scale between bound and unbound states with the same chemical shift in each state, the measured line width, LW_m, is a weighted average of the line width in the two states. The bound and unbound line widths for the receptor, LW_{bound} and $LW_{unbound}$, are weighted by the fraction of the receptor bound, f_b, as follows:

$$LW_m = f_b LW_{bound} + (1 - f_b) LW_{unbound} \quad (3)$$

The fraction of the receptor bound is dependent upon the concentration of WGA and the binding constant between WGA and the receptor. To determine the binding constant, the concentration of WGA in the sample which is available for binding to the receptor can be systematically varied by addition of a competitor which also binds WGA. In this case, the concentration of bound receptor will also depend upon the concentration of the competitor and the binding constant between the competitor and WGA. Since the WGA dimer contains multiple carbohydrate binding sites, a number of different WGA/receptor and WGA/competitor complexes may be formed. The concentrations of WGA species bound to multiple ligands will therefore depend upon higher powers of free ligand concentrations. Assuming that each WGA dimer has four receptor binding sites and that these sites are identical and noncooperative, f_b may be expressed as follows:

$$f_b = \frac{4[P]_T K_R (1 - f_b)[1 + K_R[R]_T(1 - f_b)]^3}{(1 + K_C[C])^4 + [1 + K_R[R]_T(1 - f_b)]^4 - 1} \quad (4)$$

where K_C and K_R are the dissociation constants of the competitor/lectin and receptor/lectin complexes, respectively, and [C] is the concentration of the free competitor sugar. $[R]_T$ and $[P]_T$ are the total receptor and protein concentrations, respectively. The assumption of noncooperative sites with equal affinity is supported by previous solution work (Kronis & Carver, 1985b). However, the sites do appear to exhibit some positive cooperativity when binding to cell surfaces (Lovrien & Anderson, 1980). Equation 4 should still be suitable for determining an approximate binding constant. If excess competitor sugar is present in the sample, [C] may be approximated by the total concentration of the competitor, $[C]_T$. Using this approximation and assuming that the dissociation constant of the competitor/lectin complex is known, eqs 3 and 4 contain only the unknowns K_R and the bound line width.

Since greater than stoichiometric concentrations of WGA could not be stably incorporated into the sample of the four-spacer receptor, the bound line width could not be measured directly with confidence. Therefore, a lower limit of 160 Hz for the line width of the four-spacer receptor bound to WGA was determined by measuring the line width of the receptor with half the stoichiometric concentration of WGA and extrapolating to the line width of the saturated receptor, assuming a vanishingly small dissociation constant. The lower limit will be within 50% of the true bound line width, if the dissocation constant for the WGA/receptor complex is 1 mM or less. The measured dissocation constant for *N*-acetylglucosamine complexed to wheat germ agglutinin is in fact 0.7 mM at 4 °C (Nagata & Burger, 1974).

An appropriate competitor sugar is also required to determine the dissociation constants of the receptors using eqs 3 and 4. A weak competitor is required to ensure that the experiments can be conducted using an excess of competitor. If it binds too weakly, however, unreasonably high concentrations of competitor will be required to produce an effect. Sialic acid appeared to be an appropriate selection since studies comparing the inhibition of agglutination of lipid vesicles and mammalian cells by various carbohydrates demonstrate that sialic acid binds between 2-fold and an order of magnitude less strongly to WGA than *N*-acetylglucosamine (Bhavanandan & Katlic, 1979; Monsigny et al., 1980; Redwood & Polefka, 1976). Furthermore, the dissociation constant of sialyllactose, a trisaccharide composed of lactose and sialic acid, was determined by NMR methods to be 5.7 mM at 42 °C (Kronis & Carver, 1985a).

Equations 3 and 4 may be solved numerically for the measured line width as a function of the total concentration of competitor sugar, $[C]_T$, and the dissociation constant, K_R. Figure 7 shows plots of the line width as a function of $[C]_T$ for three values of K_R between 0.025 and 2.5 mM, assuming K_C = 5 mM. The black dots are experimentally determined line widths from INADEQUATE spectra of the four-spacer receptor with various concentrations of the sialic acid competitor. The experimental points all fall near the calculated values of the line widths for K_R = 0.25 mM. This value is near that estimated for *N*-acetylglucosamine binding to WGA in solution. The binding of the two- and three-spacer receptors was reversed completely by near stoichiometric concentrations of sialic acid, demonstrating that, under these conditions, the association of WGA with the two- and three-spacer receptors is less favorable than with sialic acid in solution.

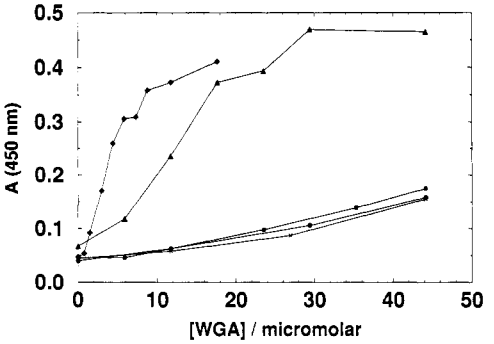

FIGURE 7: Line width of the ^{13}C-labeled carbonyl resonance of the four-spacer receptor in a DMPC/CHAPSO sample with 0.32 mM WGA dimer as a function of the concentration of sialic acid. The lines show calculated line widths as described in the text, with the dashed line, solid line, and dotted line corresponding to values of the dissociation constant between sialic acid and the receptor, K_R, of 0.025, 0.25, and 2.5 mM, respectively. The dissociation constant of the competitor and receptor is assumed to be 5 mM. The black dots are experimental values for the line width measured at different sialic acid concentrations.

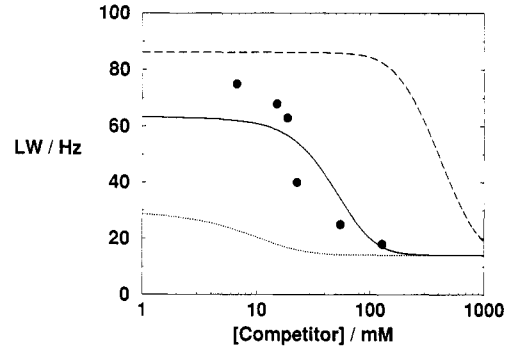

FIGURE 8: Agglutination of a 1-mL sample with 100 μg of vesicles containing 5 mol % of (◆) four-spacer receptor, (▲) three-spacer receptor, (■) two-spacer receptor, (●) one-spacer receptor, or (×) zero-spacer receptor by addition of wheat germ agglutinin. Agglutination is assayed by measuring the absorption of visible light. WGA concentrations refer to WGA dimer.

There are several possible reasons for deviation of the experimental points from line widths calculated using eq 4. In addition to difficulties in measuring bound line width, the affinity of sialic acid for each of the multiple ligand binding sites on WGA may not be the same (Wright, 1992). If the bound line width of the receptor is different for different sites, then preferential binding of sialic acid to certain sites would cause the average bound line width of the receptor to vary as a function of sialic acid concentration and the data would not fit a single value for the bound line width throughout the range of competitor concentrations studied.

Vesicle Agglutination Studies. Our NMR data show that binding constants between the receptors and WGA decrease as the *N*-acetylglucosamine headgroup is brought closer to the membrane and that the headgroups of the zero- and one-spacer receptors do not interact with WGA at all when incorporated into the DMPC/CHAPSO sample. The DMPC/CHAPSO medium might be viewed as atypical of many membrane preparations, so it is useful to make a comparison to binding properties in a pure lipid medium. To do this, we used an agglutination assay to study the interaction of WGA with the receptors incorporated in unilamellar DMPC vesicles in solution. Binding of the lectin to the ligand incorporated in the vesicles causes the vesicles to aggregate, resulting in an increase in the turbidity of the vesicle solution. Figure 8 shows the turbidity of the solutions of vesicles, each containing 5 mol % of one of the receptors, after incubation with various concentrations of WGA. WGA induces agglutination only for the vesicles incorporating the three- and four-spacer receptor. WGA also induced agglutination of DMPC vesicles containing the two-spacer receptor, but only after concentrations of receptors were raised to 14 mol %. These results are similar to the results of our NMR experiment.

One additional concern is the mode of WGA–receptor interaction. Our NMR and agglutination results are consistent with WGA interacting with the headgroups of the receptors and the alkyl chains remaining firmly anchored in the bilayers. However, the observations could also be explained by the lectin pulling the receptors out of the bilayers. If this were occurring, the bound headgroup would tumble isotropically with the protein, explaining the lack of order observed by NMR. Also, the DMPC vesicles would be destabilized by the removal of the receptors, which might cause them to fuse into larger aggregates. These would scatter light effectively and may be indistinguishable from agglutinated vesicles in the vesicle agglutination assay.

In order to determine whether a significant proportion of the receptors was being removed from the lipid bilayers by the lectin, we used ultracentrifugation to separate the lipid phase from the aqueous phase in 1-mL samples containing 100 μg of WGA and 1 mg of vesicles incorporating 5 mol % of the four-spacer receptor or zero-spacer receptor. We then assayed the aqueous phase for WGA by measuring the UV absorption spectrum between 220 and 350 nm. Because some unilamellar vesicles still remained in the aqueous phase, we fit the spectrum to a linear combination of the absorption spectra of 100 μg of WGA alone and 1 mg of DMPC vesicles alone. The best fit for the four-spacer receptor is with 33 μg of WGA in the aqueous phase. The best fit for the zero-spacer receptor is with 86 μg of WGA in the aqueous phase. These results demonstrate that a substantial fraction of WGA associates with the lipids only when a receptor which binds WGA is in the sample.

In an independent experiment, we also attempted to determine whether the small fraction of WGA remaining suspended in a centrifuged sample carried a glycolipid receptor. A 15-mL sample containing 4.5 mg of WGA and 45 mg of DMPC vesicles with 14 mol % of the four-spacer receptor was subjected to ultracentrifugation, and the aqueous phase was concentrated for NMR observation. A 1D ^{13}C NMR spectrum versus a known amount of C1-labeled mannose showed that less than 5% of the four-spacer receptor remained in the aqueous phase. Since our removal of vesicles by ultracentrifugation is seldom more than 90% complete, it is likely that the receptor observed is largely from residual vesicles and relatively little is associated with freely soluble protein. The other receptors, which are even less hydrophilic than the four-spacer receptor, are expected to be even more strongly associated with membrane systems. Although the DMPC/CHAPSO discs used in our NMR experiment are compositionally somewhat different, it is also likely that the receptors remain anchored in these systems and perturbations observed on addition of WGA are due to effects of WGA on the receptor embedded in the lipid bilayer.

DISCUSSION

The set of *N*-acetylglucosamine receptors for WGA synthesized in this study are thus demonstrated to provide a useful basis for investigating the effect of the membrane surface on the conformation of the receptors and on receptor–lectin interactions. They display a range of interactions with both

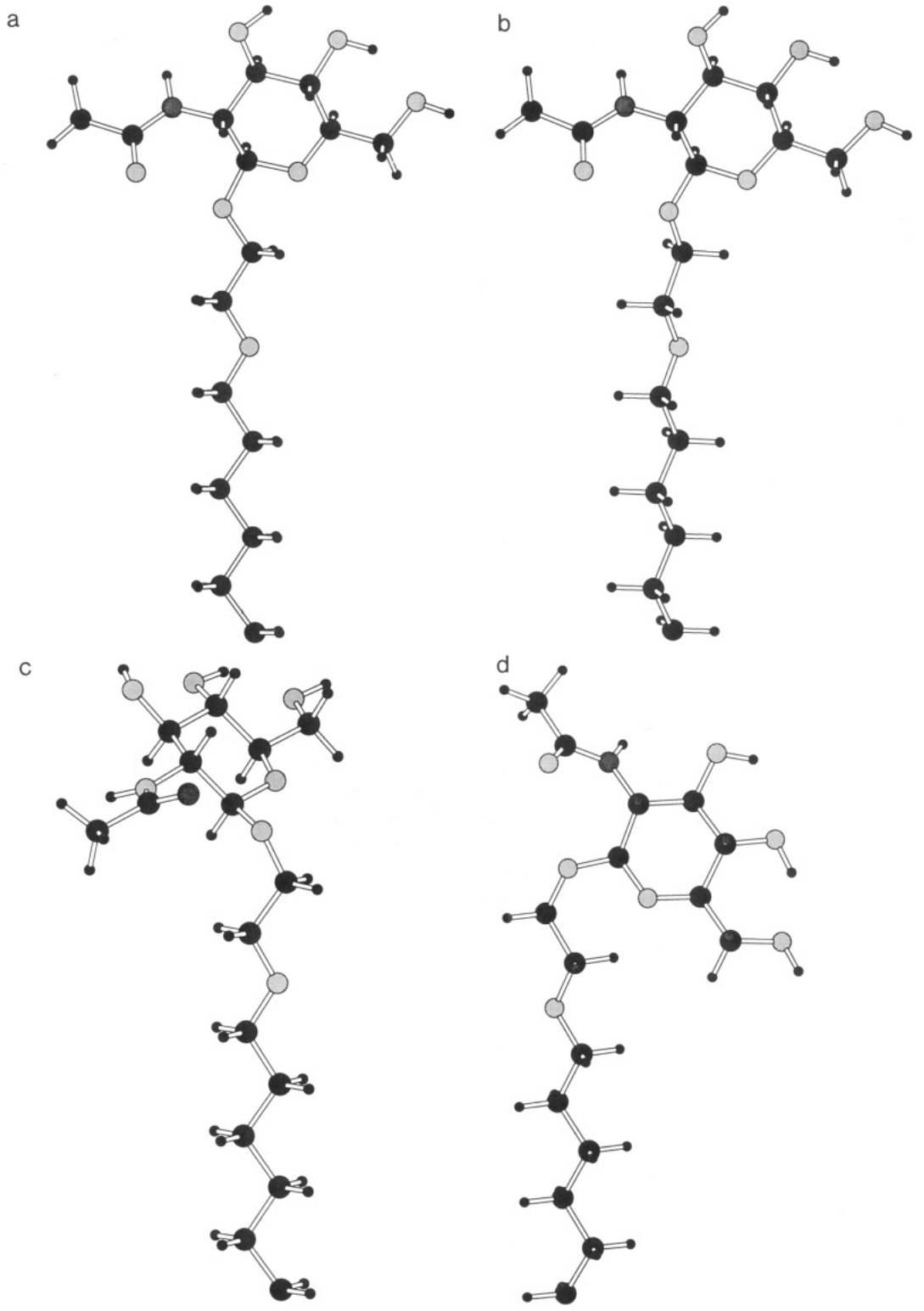

FIGURE 9: Average orientations of the one-spacer receptor which are consistent with experimental data and with low energies from molecular modeling are shown in panels a–c. The structure shown in panel a is nearly the same as the structure which molecular modeling suggests is the lowest-energy structure. The orientation of the receptor shown in panel d is suitable for binding WGA without causing the lectin/receptor complex to protrude into the membrane.

the membrane surface and the lectin. Incorporating a doubly ^{13}C-labeled *N*-acetyl substituent synthetically into *N*-acetylglucosamine as a structural probe of the headgroup at the surface of phospholipid bilayers proves very useful. It is simple and provides a modest amount of structural information. A ^{13}C–^{13}C dipolar coupling and ^{13}C carbonyl chemical shift anisotropy were used in this study. While this is not enough data to uniquely determine the orientation and order of the headgroup, it is sufficient to find sets of orientational and motional parameters which are consistent with the experimental data.

The results of the structural studies on the zero- and one-spacer receptors incorporated in the DMPC/CHAPSO bilayers demonstrate that the headgroups of these molecules are significantly ordered by the bilayers. The order parameters, S_{axial}, for the experimental solutions near the minima of the potential energy map range from 0.15 to 0.75. The corresponding order parameters for the zero-spacer receptor

are somewhat higher, suggesting a greater degree of order for the headgroup closer to the bilayer. The order parameters for both receptors are close to the axially symmetric order parameter of 0.38 ± 0.05 determined for a unique set of solutions for β-dodecyl glucoside from a much larger set of data (Hare et al., 1993).

The experimental data collected on the one-spacer receptor in the oriented lipid samples, combined with molecular modeling, may be used to discriminate among average conformations of the headgroup at the surface of the DMPC/CHAPSO micelles. The potential energy map in Figure 5 identifies five conformational regions with energies within 2 kcal/mol of the energy of the most stable conformation. The average conformations which are consistent with the experimental data cluster mainly about three of the five regions. These regions are centered at $\phi = -60°$, $\psi = 180°$, $\phi = 60°$, $\psi = 180°$, and $\phi = -60°$, $\psi = 300°$.

Among the conformations which are consistent with the experimental data, only the average structure with $\phi = -60°$ and $\psi = 160°$ has an energy within 1 kcal/mol of the energy of the apparent global-minimum conformation. This structure is shown in Figure 9a. The structure is very close to the unique conformation for β-dodecyl glucoside which is consistent with experimentally measured dipolar and quadrupolar coupling constants in the oriented DMPC/CHAPSO system (Sanders & Prestegard, 1991). Adoption of a similar structure by the *N*-acetylglucosamine headgroup in receptors separated by zero or one oxyethylene spacers from the bilayer surface would suggest that the addition of the *N*-acetyl group does not radically alter the conformational properties of glucose at a membrane surface. Our molecular modeling, however, cannot accurately differentiate between structures which differ in energy by as little as 1 or 2 kcal/mol, so experimental solutions at $\phi = 40°$, $\psi = 180°$ and $\phi = -80°$, $\psi = 270°$ cannot be ruled out. These conformations are shown in Figure 9, panels b and c, respectively. They also have reasonably extended headgroups with the *N*-acetyl group of the structure in Figure 9b nearly parallel to the bilayer surface, and with the *N*-acetyl group in the structure shown in Figure 9c tilted slightly toward the membrane. It is noteworthy that average structures with the *N*-acetyl group directed away from the membrane are not observed experimentally, since this has important implications for our observations on interaction with WGA.

We first note that the plant lectin WGA could be introduced into the DMPC/CHAPSO samples without altering the either the orientation or the order of the lipid micelles themselves. Any changes in spectral parameters of the receptor after addition of the lectin can then be interpreted as a change in the orientation or order of the receptor in a straightforward manner. We also note that WGA interacted with the same set of receptors in the DMPC/CHAPSO samples as in a much less concentrated, pure lipid medium. This is an important control experiment since it shows that intermolecular interactions observed in the DMPC/CHAPSO system probably do not strongly reflect effects of the detergent or micelle packing.

The competition studies showed weaker affinity of WGA for the three- and two-spacer receptor than the four-spacer, and no interaction was seen in either the NMR or vesicle-agglutination experiments between WGA and the zero- or one-spacer receptors. The results suggest that WGA does not interact favorably with the membrane when it binds its cell-surface ligands. Other lectin/receptor complexes may behave similarly, since vesicle-agglutination studies have shown that plant lectins often only bind carbohydrates significantly extended from a vesicle surface (Slama & Rando, 1980; Sundler, 1984). The progressively weaker affinity of the receptor headgroups for WGA as the headgroups approach the membrane may result from a decrease in entropy due to loss of conformational freedom for complexes closer to the bilayer. Alternatively, unfavorable steric interactions between the phospholipid bilayer and the lectin/receptor complex may destabilize complexes closer to the surface of the bilayer.

Evidence that complexes between WGA and the *N*-acetylglucosamine headgroups of the zero- and one-spacer receptors would be destabilized by unfavorable steric interactions with the membrane is provided by modeling the WGA/receptor complex at a membrane surface using structural information presented here. Comparisons of crystal structures of WGA complexed with carbohydrates terminating with either *N*-acetylglucosamine or sialic acid show that the *N*-acetyl group and pyranose ring of both monosaccharides superimpose almost exactly in the primary binding site (Wright, 1980). The orientation of *N*-acetylglucosamine in the binding site may therefore be approximated by overlaying the *N*-acetyl group and the ring oxygen of *N*-acetylglucosamine with the corresponding functionalities of the sialic acid found in the binding site of the high-resolution crystal structure (Wright, 1990).

Modeling of WGA bound to the one-spacer receptor incorporated in a lipid bilayer, as described above, shows that the orientation of the vector between the methyl carbon and the amide nitrogen must be roughly 45° relative to the bilayer normal in order to avoid protrusion of the lectin/receptor complex into the membrane. Figure 9d shows an energetically favorable conformation with torsion angles of $\phi = -60°$ and $\psi = 60°$. As shown in Figures 9a–c, however, the *N*-acetyl groups of conformations in regions of the energy map which are consistent with experimental data are nearly parallel to the membrane surface or tilt slightly toward the surface. Thus, our data indicate that conformations of the zero- and one-spacer receptors likely to be populated at the membrane surface are not compatible with binding to WGA. As the *N*-acetylglucosamine is extended from the surface, the conformations which it can adopt are less restrained by the membrane. In addition, the protein may be far enough away from the membrane surface to avert unfavorable contacts when it binds a variety of receptor conformations.

CONCLUSIONS

The methods described here may be suitable for studying other protein/carbohydrate complexes at a membrane surface. Although binding of wheat germ agglutinin does not appear to significantly alter the conformational properties of its ligands, it is possible that other proteins, which are known to interact with the membrane, may induce orientational preferences. These induced preferences, which may be relevant to the biological function of membrane surface receptors, may be studied using the NMR methods presented here.

REFERENCES

Aubin, Y., & Prestegard, J. H. (1993) *Biochemistry 32*, 3422–3428.
Bhavanandan, V. P., & Katlic, A. W. (1979) *J. Biol. Chem. 254*, 4000–4008.
Bush, C. A. (1992) *Curr. Opin. Struct. Biol. 2*, 655–660.
Drickamer, K. (1988) *J. Biol. Chem. 263*, 9557–9560.
Drickamer, K. (1993) *Curr. Opin. Struct. Biol. 3*, 393–400.
Feizi, T. (1985) *Nature 314*, 53–57.
Hakomori, S. (1991) *Curr. Opin. Immunol. 3*, 646–653.

Hampton, R. Y., Holz, R. W., & Goldstein, I. J. (1980) *J. Biol. Chem. 255*, 6766–6771.
Hare, B. J., Howard, K. P., & Prestegard, J. H. (1993) *Biophys. J. 64*, 392–398.
Heidlas, J., Lees, W. J., Pale, P., & Whitesides, G. M. (1992a) *J. Org. Chem. 57*, 152–157.
Heidlas, J., Lees, W. J., Pale, P., & Whitesides, G. M. (1992b) *J. Org. Chem. 57*, 146–151.
Henry, G. D., & Sykes, B. D. (1992) *Biochemistry 31*, 5284–5297.
Hoekstra, D., & Düzgunes, N. (1989) in *Artificial and Reconstructed Membrane Systems* (Harris, J. R., & Etémadi, A.-H., Eds.) Subcellular Biochemistry Vol. 14, pp 229–278, Plenum Press, New York.
Homans, S. W., & Rutherford, T. (1993) *Biochem. Soc. Trans. 21*, 449–455.
Hughes, R. C. (1992) *Curr. Opin. Struct. Biol. 2*, 687–692.
Ketchem, R. R., Hu, W., & Cross, T. A. (1993) *Science 261*, 1457–1460.
Kjellen, L., & Lindahl, U. (1991) *Annu. Rev. Biochem. 60*, 443–475.
Kronis, K. A., & Carver, J. P. (1985a) *Biochemistry 24*, 834–840.
Kronis, K. A., & Carver, J. P. (1985b) *Biochemistry 24*, 826–833.
Ladisch, S., Becker, H., & Ulsh, L. (1992) *Biochim. Biophys. Acta 1125*, 180–188.
Lasky, L. A. (1992) *Science 258*, 964–969.
Lingwood, C. A. (1992) *Curr. Opin. Struct. Biol. 2*, 693–700.
Lis, H., & Sharon, N. (1991) *Curr. Opin. Struct. Biol. 1*, 741–749.
Lovrien, R. E., & Anderson, R. A. (1980) *J. Cell Biol. 85*, 534–538.
Mayadas, T. N., Johnson, R. C., Rayburn, H., Hynes, R. O., & Wagner, D. D. (1993) *Cell 74*, 531–554.
Mo, F., & Jensen, L. H. (1975) *Acta Crystallogr., Sect. B 31*, 2867–2873.
Monsigny, M., Roche, A.-C., Sene, C., Maget-Dana, R., & Delmotte, F. (1980) *Eur. J. Biochem. 104*, 147–153.
Nagata, Y., & Burger, M. (1974) *J. Biol. Chem. 249*, 3116–3122.
Oas, T. G., Hartzell, C. J., McMahon, T. J., Drobny, G. P., & Dahlquist, F. W. (1987) *J. Am. Chem. Soc. 109*, 5956–5962.
Pardi, A., Billeter, M., & Wüthrich, K. (1984) *J. Mol. Biol. 180*, 741–751.
Pearlman, D. A., Case, D. A., Caldwell, J. C., Seibel, G. L., Singh, C., Weiner, P., Kollman, P. A. (1991) AMBER 4.0, University of California, San Francisco.
Plateau, P., & Guéron, M. (1982) *J. Am. Chem. Soc. 104*, 7310–7311.
Poppe, L., Stuike-Prill, R., Meyer, B., & van Halbeek, H. (1992) *J. Biomol. NMR 2*, 109–136.
Ram, P., Kim, E., Thomson, D. S., Howard, K. P., & Prestegard, J. H. (1993) *Biophys. J. 63*, 1530–1535.
Redwood, W. R., & Polefka, T. G. (1976) *Biochim. Biophys. Acta 455*, 631–643.
Sanders, C. R., Hare, B. J., Howard, K., & Prestegard, J. H. (1994) *Prog. Nucl. Magn. Reson. Spectrosc.* (in press).
Sanders, C. R., & Prestegard, J. H. (1990) *Biophys. J. 58*, 447–460.
Sanders, C. R., & Prestegard, J. H. (1991) *J. Am. Chem. Soc. 113*, 1987–1996.
Sanders, C. R., & Prestegard, J. H. (1992) *J. Am. Chem. Soc. 114*, 7096–7107.
Sauter, N. K., Hanson, J. E., Glick, G. D., Brown, J. H., Crowther, R. L., Park, S.-J., Skehel, J. J., & Wiley, D. C. (1992) *Biochemistry 31*, 9609–9621.
Scarsdale, J. N., Ram, P., & Prestegard, J. H. (1988) *J. Comput. Chem. 9*, 133–147.
Sharon, N., & Lis, H. (1993) *Sci. Am.*, 82–89.
Shon, K.-J., Kim, Y., Colnago, L. A., & Opella, S. J. (1991) *Science 252*, 1303–1305.
Slama, J. S., & Rando, R. R. (1980) *Biochemistry 19*, 4595–4600.
Still, W. C., et al. (1990) Macromodel V3.1, Department of Chemistry, Columbia University, New York.
Strömberg, N., Nyholm, P.-G., Pascher, I., & Normark, S. (1991) *Proc. Natl. Acad. Sci. U.S.A. 88*, 9340–9344.
Sundler, R. (1984) *Biochim. Biophys. Acta 771*, 59–67.
Vyas, N. K. (1991) *Curr. Opin. Struct. Biol. 1*, 732–740.
Winsborrow, B. G., Brisson, J. R., Smith, I. C. P., & Jarrell, H. C. (1992) *Biophys. J. 63*, 428–437.
Wright, C. S. (1980) *J. Mol. Biol. 141*, 267–291.
Wright, C. S. (1990) *J. Mol. Biol. 215*, 635–651.
Wright, C. S. (1992) *J. Biol. Chem. 267*, 14345–14352.